The Rotational–Vibrational Spectra of HCN and DCN

A Physical Chemistry Experiment

Curtis R. Keedy
Lewis and Clark College, Portland, OR 97219

An interesting extension or alternative to the classic study of the rotational–vibrational spectra of HCl and DCl is the HCN–DCN system. The HCN–DCN study is suggested by Shoemaker et al. (*1, 2*) as an extension of the HCl–DCl experiment, but no details are given.

Unfortunately, the resolution of most dispersive IR spectrometers used in education is inadequate to study this system. Because Fourier-transform IR (FTIR) instruments are now available at moderate cost (about $20,000), there is sufficient resolution available (2 cm^{-1} or better) to study the HCN and DCN gases in detail. This experiment shows the utility of isotopic substitution for the determination of molecular bond lengths that is not appreciated in the HCl–DCl experiment.

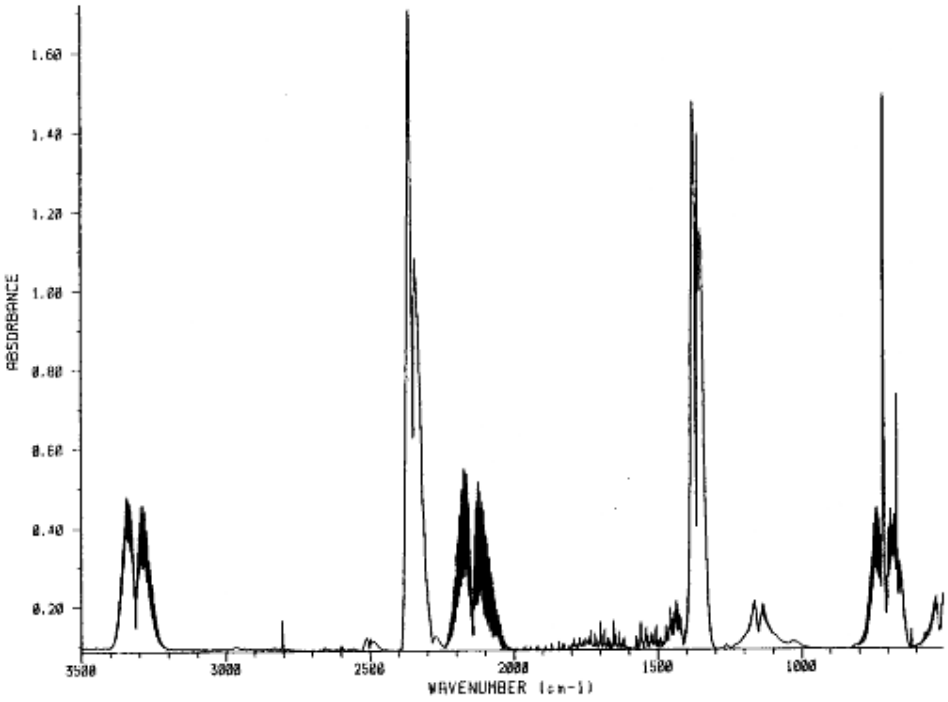

Figure 1. HCN IR spectrum showing ν_2 and ν_3 absorption bands.

Features of the HCN Spectra

Hydrogen cyanide (HCN) is a linear triatomic molecule and thus has four normal modes of vibration. In HCN these modes correspond to

ν_1 (a C–N stretch) at 2089 cm^{-1}
ν_2 (a doubly degenerate bending) at 712.1 cm^{-1}
ν_3 (a C–H stretch) at 3312 cm^{-1} (*3*)

The ν_1 mode is not IR-active, but it is Raman-active because there is little change in the molecular dipole moment during the C≡N stretch. However, the polarizability of the π electrons changes dramatically during this stretching vibration. The ν_2 mode is IR-active, but it gives rise to a perpendicular band. It is a $\Pi \leftarrow \Sigma^+$ transition. Thus, P, Q, and R branches are allowed. The ν_3 mode is also IR-active and gives rise to a parallel band with only P and R branches ($\Sigma^+ \leftarrow \Sigma^+$ transition) (*4*).

Figure 1 shows the HCN IR absorption spectrum. Other features of the spectrum include the absorption bands at 1412 cm^{-1} and 2117 cm^{-1}, which are the $2\nu_2$ and $3\nu_2$ overtones of the ν_2 fundamental. Other absorption bands represent CO_2 and H_2O impurities in the gas.

Presented at the 43rd Northwest Regional Meeting, American Chemical Society, Spokane, WA, June, 1988.

Due to the above considerations, the ν_3 band is the best candidate for this study. For the parallel bands, ($\Sigma \leftarrow \Sigma$ transitions) $\Delta J = \pm 1$ only, so only P and R branches are allowed. Thus, they give rise to exactly the same type of rotation–vibration bands as in diatomic molecules with a $^1\Sigma$ ground state (such as HCl) (*5*). Therefore, the same equations apply to this (ν_3) band as for the HCl molecule for the analysis of the rotation–vibration fine structure.

Using the notation of Herzberg et al. (*6*) with $v' = 1$ and $v'' = 0$, we get the following.

$$\nu_R = \nu_o + (2B_e - 3\alpha_e) + (2B_e - 4\alpha_e)J - \alpha_e J^2 \qquad (1)$$
$$J = 0, 1, 2, \ldots$$

$$\nu_P = \nu_o + (2B_e - 2\alpha_e)J - \alpha_e J^2 \qquad (2)$$
$$J = 1, 2, 3, \ldots$$

Let $m = J + 1$ for the R branch and $m = -J$ for the P branch. Then

$$\nu(m) = \nu_o + (2B_e - 2\alpha_e)m - \alpha_e m^2 \qquad (3)$$

where

$$m = \ldots -2, -1, 1, 2, \ldots \qquad (m \neq 0)$$

Thus,

$$\Delta\nu(m) = \nu(m+1) - \nu(m) = (2B_e - 3\alpha_e) - 2\alpha_e m \qquad (4)$$

Plotting $\Delta\nu(m)$ vs. m yields $-2\alpha_e$ as the slope and $2B_e - 3\alpha_e$ as the 0 intercept.

From B_e, the moment of inertia of the molecule can be determined.

$$B_e = \frac{h}{8\pi^2 I_e c} \qquad (5)$$

For a linear triatomic molecule,

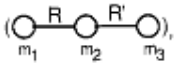

$$I_e = \frac{m_1 m_3}{M}(R+R')^2 + \frac{m_2}{M}(m_1R^2 + m_3R'^2) \qquad (6)$$

$$M = m_1 + m_2 + m_3$$

where m_1, m_2, and m_3 are the atomic masses (known); and R and R' are the bond lengths (unknown) (*7*).

Because there are two unknowns, a second determination of I_e is necessary—one for HCN and one for DCN. As verified by the HCl–DCl experiment, there is virtually no change in bond length upon isotopic substitution. Then the two equations can be solved simultaneously for R and R'.

Specifically, if atom 1 = H or D, atom 2 = C, and atom 3 = N, then we get the following.

$$I_e^{HCN} = \frac{m_H m_N}{M_{HCN}}(R+R')^2 + \frac{m_C}{M_{HCN}}(m_H R^2 + m_N R'^2) \qquad (7)$$

$$I_e^{DCN} = \frac{m_D m_N}{M_{DCN}}(R+R')^2 + \frac{m_C}{M_{DCN}}(M_D R^2 + m_N R'^2) \qquad (8)$$

Solving eqs 7 and 8 simultaneously for R', we get

$$R'^2 = \left(\frac{M_{HCN} I_e^{HCN}}{m_H m_C m_N} - \frac{M_{DCN} I_e^{DCN}}{m_D m_C m_N}\right)\left(\frac{m_H m_D}{m_D - m_H}\right) \qquad (9)$$

where R' is the square root of the right side of eq 9. R can be determined by plugging R' into eq 7 or eq 8 and solving the resulting equation for R.

Experimental Procedure

- ***Caution***: HCN is an extremely poisonous gas, and it should be handled with great care. It is colorless and has the odor of bitter almonds. All operations involving generation of the gas and handling of the gas IR cell must be carried out in a well-functioning hood. To protect the KBr windows of the gas cell and confine possible HCN leaks, the cell should be placed in a desiccator in a hood when the HCN is generated and transported to the FTIR instrument in the desiccator.
- ***Caution***: The process of generating HCN gas should be directly supervised by an experienced laboratory instructor. Alternatively, the instructor can generate a somewhat larger amount of gas in a 500-mL flask. Then students can transfer the gas in the IR cell by a vacuum transfer technique.

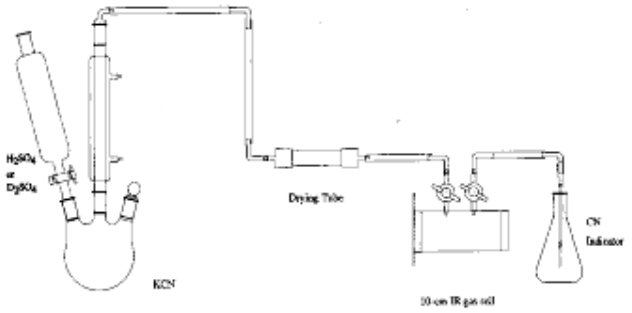

Figure 2. Experimental setup.

The HCN and DCN can be generated following the technique of Brauer (*8*). The reaction used to produce HCN was

$$2KCN(s) + H_2SO_4(concd) \rightarrow K_2SO_4 + 2HCN(g) \qquad (13)$$

To produce DCN,

$$2KCN(s) + D_2SO_4(concd) \rightarrow K_2SO_4 + 2DCN(g) \qquad (14)$$

A sketch of the apparatus used is in Figure 2.

Concentrated H_2SO_4 or D_2SO_4 (Aldrich 17,679-6) was added to solid reagent-grade KCN in the 3-neck round-bottom flask. H_2O or D_2O was removed from the gas by the $CaSO_4$ in the drying tube.

Since 1.0 g KCN will generate about 200 mL of HCN gas at 1 atm, H_2SO_4 was added in about 0.5-mL aliquots to about 2.0 g of KCN. (The volume of the 10-cm gas cell is about 200 mL.) After 2 mL of the H_2SO_4 was added, the mixture was heated if necessary to drive off the HCN. Since the boiling point of HCN is 26 °C, cooling water is not needed in the condenser.

The gas flowed through the 10-cm demountable IR gas cell fitted with KBr windows. Then it was bubbled through a cyanide indicator solution ($FeSO_4$, $Fe_2(SO_4)_3$; 1.0 M each). When the indicator solution changed from yellow/tan to deep red, CN^- was present and could be verified by observing the "Prussian Blue" color (due to $Fe_3[Fe(CN)_6]_2$) upon addition of a few drops of NH_3 solution.

At this point, the IR cell stopcocks were closed, and the heat was removed. Then the IR cell was placed in a desiccator. The outlet tubing from the reaction vessel was placed in a beaker of H_2O to reduce HCN fumes.

The FTIR spectra were taken with a Nicolet IR/32 FTIR spectrometer interfaced with an IBM 9000 computer. A background was taken after purging the cell compartment with N_2 gas for about 10 min at a resolution of 1 or 2 cm^{-1}. The IR cell containing the HCN or DCN was then placed in the spectrometer to obtain the spectrum used for analysis. Often the gas generated by the D_2SO_4 addition was sufficient to analyze both HCN and DCN lines due to water vapor in the system.

Results and Discussion

The ν_3 bands for HCN and DCN appear at about 3310 cm^{-1} and about 2630 cm^{-1}, respectively. Figures 3 and 4 are expansions of those two regions and clearly show the rotational fine structure. In fact, more than 20 lines are apparent in each of the R and P branches. The location of these absorption maxima were determined with a "peak find" routine available in the software.

The m values were assigned starting with $m = 1$ in the R branch, and $m = -1$ in the P branch, beginning at the central absorption minimum. The values of $\Delta\nu(m)$ were calculated, and $\Delta\nu(m)$ vs. m was plotted. (See Figs. 5 and 6). The

(Continued on page A298)

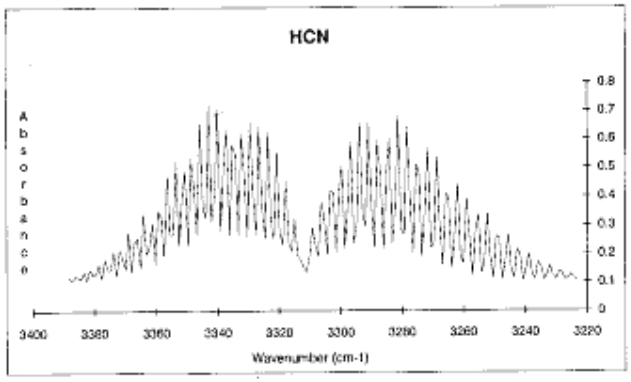

Figure 3. HCN ν_3 absorption band (expanded) at 2 cm^{-1} with boxcar apodization to increase resolution.

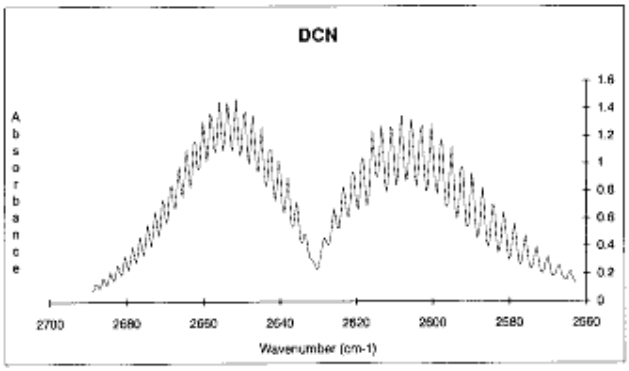

Figure 4. DCN ν_3 absorption band (expanded) at 1 cm^{-1} with Happ–Genzel apodization to improve peak shape.

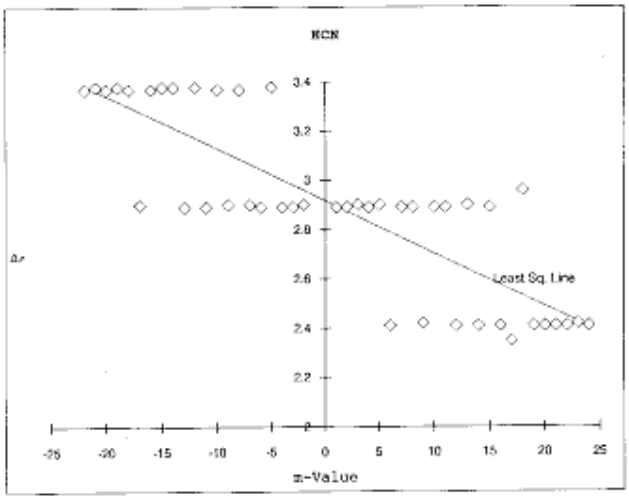

Figure 5. Plot of $\Delta\nu$ (cm^{-1}) vs. m for HCN at 1 cm^{-1} resolution.

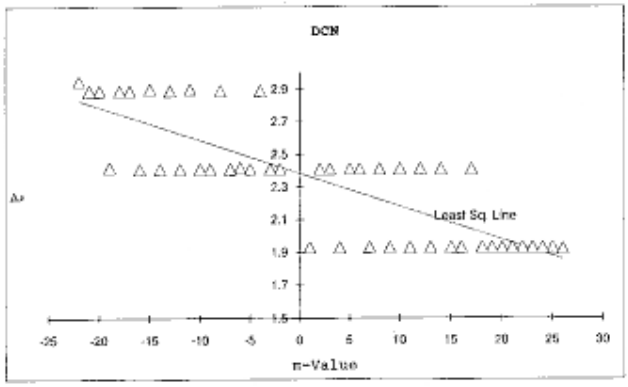

Figure 6. Plot of $\Delta\nu$ (cm^{-1}) vs. m for DCN at 1 cm^{-1} resolution.

points do not lie on the least-squares line due to the digital nature of the FTIR spectrum stored in the computer and the limitation on resolution. There is a data point every 0.5 or 1.0 cm^{-1} depending on the resolution (1 cm^{-1} or 2 cm^{-1}).

The slope and intercept of the least-squares line does yield excellent agreement with the literature data. (See the table.) The errors listed are due to scatter in the data and the resulting uncertainty in the linear regression analysis. A spreadsheet program such as SuperCalc5 or Excel is very useful in tabulating, analyzing, and graphing the data.

The values obtained are typically within 1% of the literature values. This demonstrates the validity (and necessity) of using the linear regression analysis on the digitally stored data.

Determining the moments of inertia for both HCN and DCN is necessary to solve for the bond lengths of H–C and C≡N. The isotopic substitution technique is frequently used in molecular spectroscopy for determining bond lengths, and this system is a good example. This experiment has been tested in the physical chemistry laboratory for three years at 2 cm^{-1} and 1 cm^{-1} resolution and has worked reliably.

Acknowledgment

The contributions of Michael Absalon, Sam Whiting, and Marvin Gray to this work are appreciated. The funding for the FTIR instrument was obtained from NSF–CSIP with matching funds from Lewis and Clark College.

Literature Cited

1. Shoemaker, D. P.; Garland, C. W.; Steinfeld, J. I.; Nibler, J. W. *Experiments in Physical Chemistry*, 4th ed.; McGraw–Hill: New York, 1981; p 447.
2. Shoemaker, D. P.; Garland, C. W.; Nibler, J. W. *Experiments in Physical Chemistry*, 5th ed.; McGraw–Hill: New York, 1989; p 476.
3. Herzberg, G. *Molecular Spectra and Molecular Structure II. Infrared and Raman Spectra of Polyatomic Molecules*; Van Nostrand Reinhold: Princeton, NJ, 1945; p 174.
4. Herzberg, G. *Molecular Spectra and Molecular Structure II. Infrared and Raman Spectra of Polyatomic Molecules*; p 279.
5. Herzberg, G. *Molecular Spectra and Molecular Structure II. Infrared and Raman Spectra of Polyatomic Molecules*; p 380.
6. Herzberg, G. *Molecular Spectra and Molecular Structure I. Spectra of Diatomic Molecules*; Van Nostrand Reinhold: Princeton, NJ, 1945; p 111 ff.
7. Atkins, P. W. *Physical Chemistry*, 2nd ed.; Freeman: San Francisco, 1982; p 574.
8. *Handbook of Preparative Inorganic Chemistry*, Vol. I, 2nd ed.; Brauer, G., Ed.; Academic Press: New York, 1963; p 658.
9. Naggle, J. H. *Physical Chemistry*, 2nd ed.: Scott Foreman, 1989; p 892.
10. Berry, Rice, and Ross *Physical Chemistry*; J. Wiley, 1980; p 343.

Comparison of Experimental and Literature Data for HCN and DCN

	HCN	Literature	DCN	Literature
B_e (cm^{-1})	1.474 ± 0.101	1.47822 (*9*)	1.2077 ± 0.109	1.2077 (*9*)
α_e (cm^{-1})	0.01067± 0.00107		0.01013± 0.00108	
I_e ($\times 10^{-46}$ kgm^2)	1.899 ± 0.122	1.896 (*9*)	2.319± 0.192	2.3179 (*9*)
ν_0 (cm^{-1})	3312	3312 (*4*)	2631	2629.3 (*4*)
R_{H-C} ($\times 10^{-10}$ m)	1.054	1.064 (*10*)		
$R_{C\equiv N}$ ($\times 10^{-10}$ m)	1.156	1.160 (*10*)		